
Validation of In Vivo Receptor Measurements Via In Vitro Radioassay: Technetium-99m-Galactosyl-Neoglycoalbumin as Prototype Model

Masatoshi Kudo, David R. Vera, Walter L. Trudeau, and Robert C. Stadalnik

Departments of Radiology and Internal Medicine, University of California, Davis, Medical Center, Sacramento, California

Hepatic binding protein (HBP) is a hepatocyte-specific receptor for serum asialoglycoproteins. The receptor also recognizes a synthetic glycoprotein that has been developed as a radiopharmaceutical, technetium-99m-galactosyl-neoglycoalbumin (^{99m}Tc -NGA). This report describes the correlation between receptor parameters measured in vivo via kinetic modeling of ^{99m}Tc -NGA and those measured by in vitro radioassay of biopsied liver tissue. Eleven patients with diffuse hepatic disease underwent percutaneous liver biopsy followed by a ^{99m}Tc -NGA functional imaging study. In vivo measurements of HBP quantity R_0 and forward binding rate constant k_b obtained from the kinetic analysis of ^{99m}Tc -NGA liver and blood time-activity data were compared to total receptor quantity and the HBP- ^{99m}Tc -NGA association constant K_A as measured by Scatchard binding assay of the biopsied tissue. The correlation coefficients between in vivo and in vitro measurements were 0.73 ($df=8$, $p=0.015$) and 0.98 ($df=8$, $p<0.01$) for R_0 and k_b , respectively. The in vivo measurements of HBP biochemistry via kinetic analysis of the radiopharmaceutical time-activity data reflect the average concentration and affinity of the receptor. This study further substantiates the validity of ^{99m}Tc -NGA as a quantitative probe for the HBP receptor.

J Nucl Med 1991; 32:1177-1182

Receptor-binding radiopharmaceuticals (1) are recognized and bound by large molecules called receptors. These macromolecules often reside at the plasma membrane of specific tissues and, after binding by a ligand, elicit a physiologic or pharmacologic effect. Receptor-binding radiotracers exist for specific functions of the brain (2-8), myocardium (9) and liver (10). Various investigators have proposed mathematical models (9,11-16) to obtain in vivo measurements of receptor number and affinity from imaging observations with these radiopharmaceuticals. These model values could provide a quantitative index for patient diagnosis and therapeutic management. Before these

radiopharmaceuticals and their kinetic models are used in the clinical setting, the validity of the kinetic analysis must be established. One step in validation is a demonstration that the model parameters representing receptor quantity and affinity correlate with independent values measured by accepted analytic techniques.

With the goal of quantitative diagnosis of hepatic disease, we have developed technetium-99m-galactosyl-neoglycoalbumin (^{99m}Tc -NGA) (17) and a complementary kinetic model (13,18). This receptor-binding radiopharmaceutical is a synthetic radioligand that is recognized by hepatic binding protein (HBP), a hepatocyte-specific receptor that binds galactose-terminated glycoproteins at the plasma membrane of hepatocytes. The resulting ligand-receptor complex is transported to lysosomes where the ligand is catabolized; the receptor is subsequently recycled to the cell surface and reused (19-20). Incorporated into our kinetic model are two parameters, $[R]_0$ and k_b , that conceptually represent the average concentration of HBP at the hepatocyte plasma membrane and the forward binding rate constant, respectively. The latter parameter is directly proportional to ligand-receptor affinity. Multiplication of an additional model parameter, V_n , by parameter $[R]_0$ yields an estimate of total receptor quantity, R_0 .

This study was designed to test the hypothesis that model parameters R_0 and k_b inferred from kinetic analysis of ^{99m}Tc -NGA time-activity data reflect the magnitude of tissue HBP quantity and the NGA-HBP affinity. We therefore tested the correlations of kinetic parameters R_0 and k_b with values of total HBP quantity and the NGA-HBP equilibrium constant measured by in vitro radioassay of hepatic tissue obtained by percutaneous biopsy immediately prior to ^{99m}Tc -NGA functional imaging.

MATERIALS AND METHODS

Patient Population

Ten patients (six males and four females; aged 29-73 yr), were imaged with ^{99m}Tc -NGA following a routine clinical percutaneous liver biopsy. The final diagnosis was based on histologic examination and included: acute hepatitis ($n=2$), chronic hepatitis ($n=3$), early primary biliary cirrhosis ($n=1$), alcoholic cirrhosis ($n=3$), and cholangiocell carcinoma ($n=1$). The ^{99m}Tc -NGA study and liver biopsy were performed on the same day ($n=6$) or

Received Oct. 23, 1989; revision accepted Nov. 13, 1990.
For reprints contact: Robert C. Stadalnik, MD, Division of Nuclear Medicine, University of California, Davis, Medical Center, 2315 Stockton Blvd., Sacramento, CA 95817.

within three days ($n=4$). Tissue for the receptor assay was placed in a polypropylene vial with a rubber-sealed screw cap (Stratedt; Princeton, NJ) and stored at -70°C . The storage time of each sample ranged from 2 to 16 mo. The protocol was approved by the University of California, Davis Human Subjects Review Committee.

In Vivo Assay

The $^{99\text{m}}\text{Tc}$ -NGA preparation (17), imaging procedure (10), and data analysis (18) have been described. The NGA used in this study contained an average galactose density of 24 galactose units per human serum albumin molecule. Based on preliminary clinical data (10), we selected a scaled molar dose of 1.8×10^{-9} mole per kilogram of body weight. This dose provided sufficient receptor occupancy to yield estimates of $[\text{R}]_0$ and k_b with high precision (13,18). Injected activity of $^{99\text{m}}\text{Tc}$ -NGA ranged from 4 to 6 mCi. Patients were imaged in the supine position under a large field of view gamma camera (ARC 3000; ADAC Laboratories, Milpitas, CA) fitted with a low-energy all-purpose parallel-hole collimator. Computer (DPS 33000; ADAC Laboratories, Milpitas, CA) acquisition of gamma camera data was for 30 min. Three minutes after injection 1.0 ml of venous blood was drawn. Time-activity curves for the heart and liver (the entire organ) were generated with the use of standard nuclear medicine software. The fraction of injected NGA per liter of plasma was calculated based on radioactivity assay of an aliquot of the injected dose and the 3-min blood sample.

Estimates of $[\text{R}]_0$ and k_b were obtained by curve-fitting patient liver and blood time-activity data to a kinetic model, as detailed in a companion paper (18). Briefly, a four-compartment model of a bimolecular reaction was used to simulate the $^{99\text{m}}\text{Tc}$ -NGA-HBP radiopharmacokinetic system. Using standard least squares techniques, the biochemical parameters of receptor concentration $[\text{R}]_0$ and forward binding rate constant k_b , as well as hepatic plasma flow F , extra-hepatic plasma volume V_e , hepatic plasma volume V_h , and a detector sensitivity coefficient σ_1 were adjusted until the simulated curves matched the heart and liver time-activity data. Total receptor quantity, $R_{0 \text{ in vitro}}$, was then calculated by multiplication of $[\text{R}]_0$ by V_h . Errors for each parameter were calculated via local identifiability analysis (13) and reported as the relative standard error.

In Vitro Assay

A NGA with a galactose density of 42 units per albumin molecule was prepared and labeled (chloramine-T) with iodine-125 for the Scatchard and reverse-binding assays (21). The ^{125}I -NGA was separated from free iodine by elution with 0.9% NaCl through G-25M Sephadex (PD-10; Pharmacia, Piscataway, NJ) and assayed for protein concentration (22). Proper ligand concentrations were obtained by dilution with filtered ($0.2 \mu\text{m}$) assay buffer (pH 7.5) containing 0.33 M NaCl, 0.01 M CaCl_2 , and 0.03 M 4-(2-hydroxyethyl)-1-piperazine-ethane-sulfonic acid (HEPES).

The in vitro binding assay was carried out under the conditions outlined by Van Lenten and Ashwell (23), with modifications to accommodate our small sample size. Frozen liver biopsy tissue weighing 3.6–10.9 mg was homogenized in 150 μl of cold acetone (-20°C) using a microsample tissue grinder (Radnoti Glass, Monrovia, CA) that had been stored at -20°C . The homogenization consisted of 10 complete strokes and 20 rotations over 5 min. After addition of 15 ml of cold acetone, the homogenate was centrifuged (Accuspin FR; Beckman Instruments, Palo Alto, CA)

at 600 G, 4°C for 15 min. The supernatant was removed and the pellet was dried by a stream of filtered air. The resulting acetone powder was reconstituted and rehomogenized in 1.2 ml of filtered assay buffer (pH 7.5) consisting of 0.33 M NaCl, 0.01 M CaCl_2 , and 0.03 M HEPES. After sampling, 20 μl of membrane suspension in triplicate for protein assay (22), 1.2 ml of filtered ($0.45 \mu\text{m}$) assay buffer containing 0.1% bovine serum albumin (BSA) (Sigma Chemical, St. Louis, MO) was added to the membrane suspension.

The Scatchard binding assay was performed by incubating 200 μl of membrane suspension in duplicate with ^{125}I -NGA at one of three initial concentrations 6.4×10^{-12} , 8.0×10^{-11} , and 1.6×10^{-10} M for 9 hr at 37°C in polypropylene tubes (12×75 mm) with gentle magnetic stirring. Final assay volume was 400 μl . A blank containing 200 μl of ^{125}I -NGA at each initial NGA concentration and 200 μl of assay buffer was also incubated under similar conditions. The membrane suspension or blank was applied to an assembly containing a $0.45\text{-}\mu\text{m}$ filter (HVLP 013; Millipore Corp., Bedford, MA) which had been soaked for 10 min in filtered ($0.45 \mu\text{m}$) assay buffer containing 0.1% BSA. Each filter assembly was then centrifuged (High Speed Centrifuge with Model HSR-16 rotor; Savant Instruments, Farmingdale, NY) at 3600 G for 10 min. The assemblies were rinsed twice by application of assay buffer (1 ml) and recentrifugation. The filters were placed in plastic 20-ml counting vials and assayed for radioactivity (20–40 keV).

Receptor concentration and affinity were calculated (see Appendix) via linear regression (24) of B/F on [B], which forms a standard Scatchard plot (25) of bound/free versus concentration bound. The equilibrium constant K_A was calculated as the negative of the slope of the regression line. Errors for slopes and y-intercepts were calculated via standard methods (24). The receptor concentration within the assay tube, $[\text{R}]_{\text{tube}}$, was determined as the y-intercept divided by K_A . Receptor concentration was converted to receptor quantity via multiplication by the assay volume. Based on an approximate liver weight of 2.2% of total-body weight (26) and the amount of membrane per assay, the total amount of HBP ($R_{0 \text{ in vitro}}$) was determined.

A final point regarding k_b pertains to our use of ^{125}I -NGA-42 (42 galactose units per albumin molecule) as the radioligand for the in vitro binding assays. This preparation had a higher carbohydrate density, and therefore a higher k_b (21) by a factor of 1.25, than the technetium-labeled NGA-24 employed in the imaging studies. Therefore, ^{125}I -NGA-42 provided Scatchard plots with greater slopes, and thus measurement values of K_A and $[\text{R}]_{\text{in vitro}}$ of higher precision. Use of [^{125}I]NGA-24 would produce more scatter in the correlation plot of k_b (see Fig. 2) and would decrease the magnitude of the in vitro measurements.

The reverse-binding assay was carried out in the following manner. The 200 μl of membrane suspension were incubated in a polypropylene tube (12×75 mm) with 200 μl of 8.0×10^{-13} M ^{125}I -NGA for 9 hr at 37°C . At this time, 100 μl of 5×10^{-8} mol/ml NGA (42 galactose units per human serum albumin) were added. At 1 and 15 hr after the addition of nonlabeled NGA, two 100- μl aliquots were applied to two filter assemblies and centrifuged (3200 G). The assemblies were then rinsed with assay buffer and recentrifuged. The filtrates and standard were counted as described above. Reverse-binding rate constant k_{-b} was calculated as the negative of the slope resulting from linear regression of $\ln(\text{fB})$ on time, where the fraction bound fB was calculated via Equation A4 (see Appendix). The forward-binding rate constant, k_b , was obtained by multiplication of K_A by k_{-b} .

TABLE 1
Patient Summary

Study no.	Age/ Sex	Diagnosis	Weight (kg)	Height (m)	Hematocrit (%)	Expected plasma volume (liter)	Expected hepatic plasma flow (liter/min ⁻¹)
1	73 M	Acute hepatitis	66	1.81	33	3.21	1.06
2	31 F	Acute hepatitis	56	1.72	38	2.34	0.84
3	52 M	Chronic hepatitis	102	1.78	32	3.92	1.67
4	39 M	Chronic hepatitis	70	1.84	44	2.88	0.97
5	46 F	Chronic hepatitis	92	1.70	41	2.70	1.32
6	42 F	Liver cirrhosis	90	1.62	21	2.70	1.67
7	29 M	Liver cirrhosis	56	1.60	33	2.61	0.89
8	37 M	Liver cirrhosis	80	1.70	39	3.03	1.18
9	65 M	Cholangiocarcinoma	93	1.80	38	3.56	1.40
10	44 F	PBC*	79	1.52	47	2.15	1.04

* Primary biliary cirrhosis.

The relative standard error for k_b ($se(k_b)$) was calculated by quadratic addition of the relative errors for K_A and $k_{in\ vitro}$ (24).

Reproducibility

Reproducibility of the in vitro assay was tested by using two surgical specimens (histologically-proven) of normal and cirrhotic livers. Membrane isolation and Scatchard assays were performed 12 times for each specimen using tissue samples with sizes similar to the percutaneous specimens.

Statistical Analysis

This study tested two null hypotheses: (1) a linear relationship between in vivo measurements of R_o via ^{99m}Tc-NGA imaging and HBP quantity from the biopsy assay does not exist, and (2) a linear relationship between in vivo measurement of k_b via ^{99m}Tc-NGA imaging and constant K_A obtained from the biopsy assay does not exist. Association was tested by calculation of the Pearson correlation coefficient following a weighted linear regression (SAS JMP; Cary, NC). The reciprocal of $se(R_{in\ vitro})^2$ or $se(K_A)^2$ was used as the weighting factor. A confidence level of 95% was used as the criterion for significance. Statistical comparison between the mean receptor density of surgically resected normal liver and cirrhotic liver was made with the Student's t-test (two-tailed, unpaired) at a confidence level of 95%. Standard

linear regression (24) was employed for Lowry, Scatchard, and reverse-binding assays. Mean and standard deviation were calculated for slopes and y-intercepts. Errors resulting from multiplication or division were assumed to propagate as the quadratic sum (24) of relative errors. Weighted linear regression was used to calculate the slope and y-intercept of each correlation plot.

RESULTS

In vitro measurements of surgical specimens detected 0.430 ± 0.041 μ mole HBP per mole of protein (mean \pm s.e.m.) in the normal liver (12 samples from a single biopsy) and 0.144 ± 0.012 μ mole HBP per mole of protein in the cirrhotic liver (12 samples from a single biopsy). The difference between the means was statistically significant ($p < 0.001$). The standard deviation of the Lowry assay was 5%. All blanks contained less than 1% of the incubated activity. Patient age, sex, weight, height, expected plasma volume (27), and hepatic plasma flow (26) are listed in Table 1.

In vitro assay and in vivo results are listed in Tables 2 and 3, respectively. Table 2 includes the amount of assayed

TABLE 2
In Vitro Binding Assay

Study no.	Liver tissue (mg)	K_A^* (nM^{-1})	k_b ($min^{-1} \times 10^4$)	$k_{b\ in\ vitro}$ ($\mu M^{-1} min^{-1}$)	$R_{o\ in\ vitro}$ (μ mole)
1	4.9	1.47 \pm (0.63)	2.41 \pm (0.38)	3.56 \pm (0.73)	0.081 \pm (0.63)
2	5.3	1.05 \pm (0.47)	3.21 \pm (0.22)	3.37 \pm (0.51)	0.058 \pm (0.47)
3	5.7	1.08 \pm (0.71)	4.53 \pm (0.11)	4.88 \pm (0.72)	0.100 \pm (0.71)
4	10.9	1.32 \pm (0.37)	2.70 \pm (0.10)	3.57 \pm (0.38)	0.029 \pm (0.37)
5	3.6	1.57 \pm (0.45)	1.79 \pm (0.01)	2.82 \pm (0.47)	0.088 \pm (0.47)
6	4.9	1.81 \pm (0.36)	1.61 \pm (0.30)	2.92 \pm (0.46)	0.031 \pm (0.36)
7	5.5	1.47 \pm (0.62)	3.55 \pm (0.08)	5.20 \pm (0.62)	0.022 \pm (0.62)
8	4.4	1.08 \pm (0.44)	3.59 \pm (0.19)	3.88 \pm (0.48)	0.070 \pm (0.44)
9	3.8	1.51 \pm (0.69)	0.42 \pm (1.28)	0.63 \pm (1.45)	0.048 \pm (0.69)
10	7.2	0.99 \pm (0.77)	4.17 \pm (0.08)	4.12 \pm (0.78)	0.081 \pm (0.79)

* Mean \pm ($se(p)/p$).

tissue, the equilibrium association constant K_A , the NGA-HBP forward-binding rate constant k_b , the reverse-binding rate constant k_{-b} , and the total receptor quantity R_o in vitro. The three latter values are reported with relative standard deviations. Table 3 lists the estimates and relative standard errors for parameters $[R]_o$, k_b , hepatic plasma flow F , and total plasma volume V_p , total receptor quantity R_o in vitro, and a measure of the systematic curve-fit error, the reduced chi-square (24). Linear correlation coefficients for the Scatchard and reverse-binding assays ranged from 0.54 to 0.82 and 0.87 to 0.99, respectively.

Correlation between model parameters and the in vitro measurements is presented in Figures 1 and 2. Error bars representing 1 s.d. are included. Variables R_o in vitro and R_o in vivo were highly correlated ($r=0.73$, $df=8$, $p=0.015$). Linear regression with R_o in vitro as the abscissa and R_o in vivo as the ordinate yielded a y-intercept and slope of $-0.007 \mu\text{mole}$ and 0.33 ± 0.13 , respectively. Model parameter k_b and the forward-binding rate constant as measured by in vitro binding assay were also significantly correlated ($r=0.98$, $df=8$, $p<0.01$). Linear regression of k_b in vitro with k_b in vivo yielded a y-intercept of zero and slope of $5 \times 10^2 \text{ min}^{-1}$, respectively. We therefore rejected each null hypothesis and concluded that in vivo estimates of R_o and k_b reflect the magnitude of receptor quantity and ligand-receptor affinity.

DISCUSSION

Rational development of receptor-binding radiopharmaceuticals can be divided into four stages. The first is a demonstration that the mechanism of localization of the new radiotracer is receptor-mediated. This has been accomplished for several radiopharmaceuticals: ^{18}F -DOPA (4), ^{125}I -3-quinuclidinyl 4-iodobenzilate (QNB) (8), ^{11}C -quinuclidinyl benzilate methiodide (MQNB) (9), ^{18}F -spiroperidol (SP) (2,5), ^{11}C -*N*-methyl-spiperone (NMSP) (3), and $^{99\text{m}}\text{Tc}$ -NGA (28,17). The second stage is a demonstra-

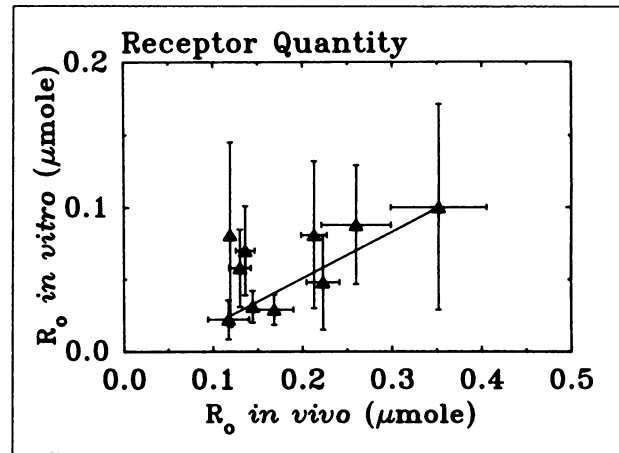


FIGURE 1. Total receptor quantity R_o correlated with the total amount of HBP as measured by in vitro assay ($r=0.73$, $df=8$, $p=0.015$). The correlation was determined by weighted ($1/\text{se}(R_o \text{ in vitro})^2$) linear regression.

tion that an alteration in biodistribution reflects a change in specific physiologic state. Studies with ^{18}F -DOPA (7), ^{125}I -QNB (6), ^{11}C -MQNB (9), ^{11}C -NMSP (12), and $^{99\text{m}}\text{Tc}$ -NGA (10) have demonstrated altered time-activity data for various disease and physiologic states. Neither of these early stages require a kinetic model.

The goal of the third stage is a validation of the method as an accurate measurement of receptor biochemistry. This stage involves several levels and incorporates a kinetic model of tracer localization. Kinetic models have been proposed and tested for ^{11}C -MQNB (9), ^{18}F -SP (11,16), ^{11}C -NMSP (12), ^{11}C -raclopride (14), and $^{99\text{m}}\text{Tc}$ -NGA (18). This requires that simulation of the model can accurately describe the tracer's time-activity data and is used to test the plausibility of the model's structure. For example, the $^{99\text{m}}\text{Tc}$ -NGA model is composed of two processes: a hemodynamic component determined by flow and volume and a biochemical component determined by a bimolecular

TABLE 3
In Vivo Assay Results*

Subject no.	$[R]_o$ (μM)	k_b in vivo ($\mu\text{M}^{-1} \text{ min}^{-1}$)	F (liter/min $^{-1}$)	V_p † (liter)	V_h (liter)	R_o in vivo‡ (μmole)	χ^2
1	0.789 ± (0.068)	2.00 ± (0.17)	1.19 ± (0.62)	1.88 ± (0.011)	0.272 ± (0.003)	0.213 ± (0.068)	1.39
2	0.672 ± (0.093)	2.85 ± (0.35)	0.75 ± (0.99)	1.41 ± (0.022)	0.194 ± (0.004)	0.130 ± (0.094)	2.74
3	0.866 ± (0.150)	2.42 ± (0.41)	1.29 ± (0.75)	3.92 ± (0.018)	0.407 ± (0.003)	0.352 ± (0.152)	1.64
4	0.849 ± (0.012)	2.51 ± (0.50)	1.16 ± (2.74)	1.29 ± (0.040)	0.197 ± (0.007)	0.168 ± (0.129)	3.01
5	0.803 ± (0.015)	2.36 ± (0.48)	1.33 ± (1.36)	2.79 ± (0.023)	0.323 ± (0.009)	0.260 ± (0.149)	2.62
6	0.362 ± (0.016)	3.61 ± (0.12)	1.51 ± (1.13)	2.45 ± (0.020)	0.397 ± (0.007)	0.144 ± (0.018)	1.49
7	0.270 ± (0.196)	2.44 ± (0.72)	0.98 ± (3.53)	1.39 ± (0.078)	0.434 ± (0.015)	0.117 ± (0.197)	6.13
8	0.402 ± (0.075)	1.93 ± (0.27)	1.18 ± (1.28)	2.89 ± (0.023)	0.337 ± (0.012)	0.136 ± (0.079)	2.11
9	0.426 ± (0.083)	3.40 ± (0.30)	1.51 ± (1.04)	3.28 ± (0.023)	0.524 ± (0.006)	0.223 ± (0.083)	1.59
10	0.697 ± (0.014)	1.88 ± (0.07)	1.12 ± (0.60)	2.11 ± (0.006)	0.171 ± (0.007)	0.119 ± (0.018)	1.63

* Mean ± (se(p)/p).

† Total plasma volume = $V_o + V_h$.

‡ R_o in vivo = $[R]_o V_h$.

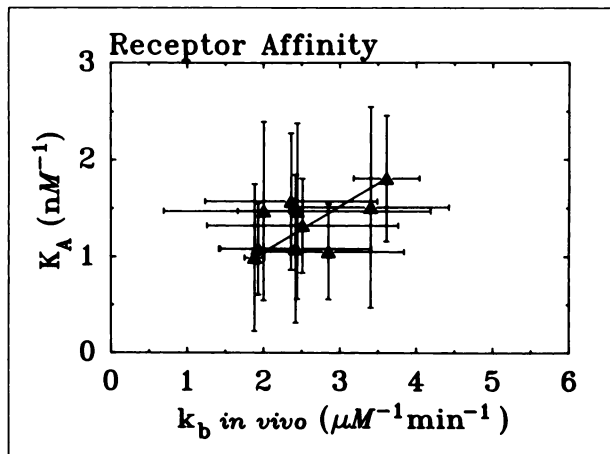


FIGURE 2. Model parameter k_b and an independent measurement of ^{99m}Tc -NGA-HBP affinity, K_A , were highly correlated ($r=0.98$, $df=8$, $p<0.01$). The x-axis error bars are smaller than the symbols. The correlation was determined by weighted $(1/\text{se}(K_A)^2)$ linear regression.

reaction. The fact that model simulations could reproduce the shape of ^{99m}Tc -NGA liver and heart time-activity data supported the hypothesis that the structure of the proposed model is a plausible representation of the actual radiopharmacokinetic system. This stage also requires a demonstration of kinetic sensitivity to the model parameters. This has been accomplished for ^{99m}Tc -NGA (29), where studies in pigs displayed changes in liver and blood time-activity data when either hepatic plasma flow, ligand-receptor affinity, or the molar dose of the ligand were altered. These observations identified those parameters as real components of a ^{99m}Tc -NGA radiopharmacokinetic system. The final level of validation is achieved when independent measurements are shown to correlate with corresponding parameters obtained from kinetic analysis of time-activity data. The model parameters should have the same units and values as the independent measurements. Therefore, a linear regression of each model parameter against the independent measurement should ideally produce a y-intercept of zero and a slope of one. The present manuscript achieves this level of validation for ^{99m}Tc -NGA.

The final stage in the rational design of a receptor-binding radiopharmaceutical is demonstration of clinical efficacy. A model that provides accurate and precise measurements of receptor biochemistry is a prerequisite for successful clinical application, but if the biochemical state of the receptor remains unchanged in disease, the imaging study will not provide adequate sensitivity as a test of tissue function. This may be the case for ^{99m}Tc -NGA-HBP k_b , which exhibited small changes according to both the in vitro assay and the ^{99m}Tc -NGA model. Additionally, the biochemical and clinical validations will differ because each may require different forms of the tested parameters. For example, we used an extensive form of the receptor parameter R_o , total receptor quantity, to test the biochemical validity of the ^{99m}Tc -NGA model. A clinically relevant

index will require an intensive variable that is independent of certain variables such as plasma volume or body weight. Therefore, clinical validation of a receptor-binding radiopharmaceutical would test parameters such as receptor concentration $[R]_o$ or receptor quantity per body weight.

In this study, we compared a measure of ligand-receptor affinity, the association constant K_A , with the model parameter k_b , which when divided by k_{-b} (assumed constant by the model) equals K_A . Calculation of k_b from in vitro assay required two separate measurements: K_A from the Scatchard assay and k_{-b} from the reverse-binding assay. The combined error of both measurements produced excessively high relative errors (0.5–1.5). As a result, the correlation of k_b in vitro with k_b in vivo was not significant. The possibility exists that k_b is not altered in diseased tissue. Therefore, the direct correlation of ^{99m}Tc -NGA-HBP k_b will require an in vitro assay of higher precision to measure the relatively small differences in k_b .

In conclusion, in vivo measurements of HBP biochemistry obtained via modeling of ^{99m}Tc -NGA dynamic imaging has been shown to correlate with in vitro assays of HBP quantity and ligand affinity. This observation further substantiates the validity of in vivo measurements of HBP biochemistry via ^{99m}Tc -NGA modeling, which is a prerequisite to the clinical validation of ^{99m}Tc -NGA functional imaging of the liver (10,30).

APPENDIX

Variables for the Scatchard assay were calculated in the following manner:

$$[B]_{ij} = \frac{\text{cpm}(F_{ij})}{\text{cpm}([L_o]_i)} [L_o]_i \quad \text{Eq. A1}$$

$$[F]_q = \frac{\text{cpm}([L_o]_i) - \text{cpm}(F_{ij})}{\text{cpm}([L_o]_i)} [L_o]_i \quad \text{Eq. A2}$$

$$B/F = [B]_{ij}/[F]_{ij}, \quad \text{Eq. A3}$$

where $[B]_{ij}$ and $[F]_{ij}$ are the bound and free concentrations of ^{125}I -NGA for the i -th initial ^{125}I -NGA concentration and the j -th replicate, $[L_o]_i$ is the i -th initial ^{125}I -NGA concentration, $\text{cpm}(F_{ij})$, is the count rate resulting from the radioassay of the filter bearing membrane-bound ^{125}I -NGA from the j -th replicate of the i -th initial ^{125}I -NGA concentration; and $\text{cpm}([L_o]_i)$ is a standard containing the i -th initial concentration of ^{125}I -NGA.

The reverse-binding assay used the variable

$$fB_{jk} = \frac{\text{cpm}(F_{jk})}{\text{cpm}([L_o]_j)}, \quad \text{Eq. A4}$$

where fB_{jk} is the fraction bound of the j -th replicate at the k -th time point.

ACKNOWLEDGMENTS

The authors thank Drs. Kenneth A. Krohn, William C. Eckelman, and Paul O. Scheibe for valuable discussions and critical reviews. We also acknowledge the excellent technical assistance of Dusan P. Hutak. This study was supported by U.S. Public Health Service grants RO1-AM34768 and RO1-AM34706 from the National Institute of Arthritis, and U.S. Department of Energy grant DE-FGO3-87ER60553.

This paper was presented at the 36th Annual Meeting of The Society of Nuclear Medicine as the 1989 Berson-Yalow award.

REFERENCES

1. Eckelman WC, Reba RC. The classification of radiotracers. *J Nucl Med* 1978;19:1179-1181.
2. Welch MJ, Kilbourn MR, Mathias CJ, Mintun MA, Raichle ME. Comparison in animal models of [¹⁸F]spiroperidol and [¹⁸F]haloperidol: potential agents for imaging the dopamine receptor. *Life Sci* 1983;33:1687-1693.
3. Wagner HN Jr, Burns HD, Dannals DF, et al. Imaging dopamine receptors in the human brain by positron tomography. *Science* 1983;221:1264-1266.
4. Garnett ES, Firnau G, Nahmias C. Dopamine visualized in the basal ganglia of living man. *Nature* 1983;305:137-138.
5. Arnett CD, Shiue C-Y, Wolf AP, Fowler JS, Logan J, Watanabe M. Comparison of three ¹⁸F-labeled butyrophenone neuroleptic drugs in the baboon using positron emission tomography. *J Neurochem* 1985;44:835-844.
6. Holman BL, Gibson RE, Hill TC, et al. Muscarinic acetylcholine receptors in Alzheimer's disease. *JAMA* 1985;254:3063-3066.
7. Calne DB, Langston JW, Martin WRW, et al. Positron emission tomography after MPTP: observations relating to the cause of Parkinson's disease. *Nature* 1985;317:246-248.
8. Eckelman WC, Reba RC, Rzeszutarski WJ, et al. External imaging of cerebral muscarinic acetylcholine receptors. *Science* 1984;223:291-293.
9. Syrota A, Comar D, Paillotin G, et al. Muscarinic cholinergic receptor in the human heart evidenced under physiological conditions by positron emission tomography. *Proc Natl Acad Sci USA* 1985;82:584-588.
10. Stadalnik RC, Vera DR, Woodle ES, et al. Technetium-99m-NGA functional hepatic imaging: preliminary clinical experience. *J Nucl Med* 1985;26:1233-1242.
11. Mintun MA, Raichle ME, Kilbourn MR, Wooten GF, Welch MJ. A quantitative model for the in vivo assessment of drug-binding sites with positron emission tomography. *Ann Neurol* 1984;15:217-227.
12. Wong DF, Wagner HN Jr, Dannals RF, et al. Effects of age on dopamine and serotonin receptors measured by positron tomography in the living human brain. *Science* 1984;226:1393-1396.
13. Vera DR, Krohn KA, Scheibe PO, Stadalnik RC. Identifiability analysis of an in vivo receptor-binding radiopharmacokinetic system. *IEEE Trans Biomed Eng* 1985;BME-32:312-322.
14. Farde L, Hall H, Ehrin E, Sedvall G. Quantitative analysis of D2 dopamine receptor binding in the living human brain by PET. *Science* 1986;231:258-261.
15. Stadalnik RC, Vera DR, Krohn KA. Receptor-binding radiopharmaceuticals: experimental and clinical aspects. In: Freeman LM, Weissmann HS, eds. *Nuclear medicine annual 1986*. New York: Raven Press; 1986:105-139.
16. Logan J, Wolf AP, Shiue C-Y, Fowler JS. Kinetic modeling of receptor-ligand binding applied to positron emission tomographic studies with neuroleptic tracers. *J Neurochem* 1987;48:73-83.
17. Vera DR, Stadalnik RC, Krohn KA. [Tc-99m]-galactosyl neoglycoalbumin: preparation and preclinical studies. *J Nucl Med* 1985;26:1157-1167.
18. Vera DR, Stadalnik RC, Trudeau WL, Scheibe PO, Krohn KA. Measurement of receptor concentration and forward-binding rate constant via radiopharmacokinetic modeling of ^{99m}Tc-galactosyl-neoglycoalbumin. *J Nucl Med* 1991;32:1169-1176.
19. Steer CJ, Ashwell G. Studies on a mammalian hepatic binding protein specific for asialoglycoproteins: evidence for receptor recycling in isolated rat hepatocytes. *J Biol Chem* 1980;255:3008-3013.
20. Stockert RJ, Morell AG. Hepatic binding protein. The galactose-specific receptor of mammalian hepatocytes. *Hepatology* 1983;3:750-757.
21. Vera DR, Krohn KA, Stadalnik RC, Scheibe PO. [Tc-99m]-galactosyl-neoglycoalbumin: in vitro characterization of receptor-mediated binding. *J Nucl Med* 1984;25:779-787.
22. Lowry OH, Rosebrough NJ, Farr AL, Randell RJ. Protein measurement with the Folin phenol reagent. *J Biol Chem* 1951;193:265-275.
23. Van Lenten L, Ashwell G. The binding of desialylated glycoproteins by plasma membranes of rat liver: development of a quantitative inhibition assay. *J Biol Chem* 1972;247:4633-4640.
24. Bevington PR. *Data reduction and error analysis for the physical sciences*, first edition. New York: McGraw Hill; 1969.
25. Scatchard G. The attractions of proteins for small molecules and ions. *Ann NY Acad Sci* 1949;51:660-672.
26. Greenway CV, Stark RD. Hepatic vascular bed. *Phys Rev* 1971;51:23-65.
27. Nadler SB, Hidalgo JU, Bloch T. Prediction of blood volume in normal adults. *Surgery* 1962;51:224-232.
28. Vera DR, Krohn KA, Stadalnik RC, Scheibe PO. [Tc-99m]-galactosyl-neoglycoalbumin: in vivo characterization of receptor-mediated binding to hepatocytes. *Radiology* 1984;151:191-196.
29. Vera DR, Woodle ES, Stadalnik RC. Kinetic sensitivity of a receptor-binding radiopharmaceutical: technetium-99m-galactosyl-neoglycoalbumin. *J Nucl Med* 1989;30:1519-1530.
30. Kudo M, Vera DR, Stadalnik RC, Trudeau WL, Ikekubo K, Toda A. In vivo estimates of hepatic binding protein concentration: correlation with classical indicators of hepatic function reserve. *Am J Gastroenterol* 1990;85:1142-1148.

EDITORIAL

A Perspective: In Vivo Assay of Receptor-Ligand Binding

Workers in nuclear medicine have repeatedly referred to the field as depending on "function" rather than on differences between tissue densities or related properties. But what aspects of function are we measuring? Most are on a macroscopic level. Results are usually reported in comparison with a standard. For example, after ingestion of ¹²³I-sodium iodide, thyroidal "uptake" is expressed as a percent of the ingested dose.

The exact amount of stable iodide accumulated by the thyroid is difficult to evaluate; the radiotracer administered is often "carrier-free." Intrathyroidal radioiodide accumulation represents the net of multiple processes, principally the difference between uptake of radiotracer and discharge of radioiodide or iodinated products. The blood stream content of stable iodide, blood flow to the thyroid, extraction, organification, storage and discharge are all occurring. Analysis of this degree of complexity is usually not attempted, although portions of the pathway can often be examined. Another

way of expressing this is that: (1) data needed to provide a full analysis are usually not available and (2) a more detailed assay may have little relevance for clinical measurement.

The two papers by Vera and co-workers (1,2) provide an approach to examining events not on a macroscopic scale, but on the microscopic level. They have provided a means of analyzing the binding of a radioactive ligand to a specific receptor (hepatic binding protein or HBP). Quantitative analysis was possible, by means of imaging, blood sampling and reasonable as-

Received Dec. 3, 1990; accepted Dec. 3, 1990.
For reprints contact: Richard P. Spencer, MD, PhD, University of Connecticut Health Center, Farmington, CT 06030.